University Library



A gateway to Melbourne's research publications

Minerva Access is the Institutional Repository of The University of Melbourne

Author/s:
Korsah, MA;Johnston, ST;Tiedje, KE;Day, KP;Flegg, JA;Walker, CR

Title:
Mathematical Assessment of the Role of Intervention Programs for Malaria Control

Date:
2024-08-01

Citation:
Korsah, M. A., Johnston, S. T., Tiedje, K. E., Day, K. P., Flegg, J. A. & Walker, C. R. (2024). Mathematical Assessment of the Role of Intervention Programs for Malaria Control. Bulletin of Mathematical Biology, 86 (8), https://doi.org/10.1007/s11538-024-01321-0.

Persistent Link:
https://hdl.handle.net/11343/353839

License:
CC BY

Bulletin of Mathematical Biology (2024) 86:91
https://doi.org/10.1007/s11538-024-01321-0

Society for Mathematical Biology

ORIGINAL ARTICLE



Mathematical Assessment of the Role of Intervention Programs for Malaria Control

Maame Akua Korsah[1] · Stuart T. Johnston[1] · Kathryn E. Tiedje[2] · Karen P. Day[2] · Jennifer A. Flegg[1] · Camelia R. Walker[1,3]

Received: 17 December 2023 / Accepted: 3 June 2024
© The Author(s) 2024

Abstract

Malaria remains a global health problem despite the many attempts to control and eradicate it. There is an urgent need to understand the current transmission dynamics of malaria and to determine the interventions necessary to control malaria. In this paper, we seek to develop a fit-for-purpose mathematical model to assess the interventions needed to control malaria in an endemic setting. To achieve this, we formulate a malaria transmission model to analyse the spread of malaria in the presence of interventions. A sensitivity analysis of the model is performed to determine the relative impact of the model parameters on disease transmission. We explore how existing variations in the recruitment and management of intervention strategies affect malaria transmission. Results obtained from the study imply that the discontinuation of existing interventions has a significant effect on malaria prevalence. Thus, the maintenance of interventions is imperative for malaria elimination and eradication. In a scenario study aimed at assessing the impact of long-lasting insecticidal nets (LLINs), indoor residual spraying (IRS), and localized individual measures, our findings indicate that increased LLINs utilization and extended IRS coverage (with longer-lasting insecticides) cause a more pronounced reduction in symptomatic malaria prevalence compared to a reduced LLINs utilization and shorter IRS coverage. Additionally, our study demonstrates the impact of localized preventive measures in mitigating the spread of malaria when compared to the absence of interventions.

Keywords Malaria · Intervention programs · Mathematical modelling · Sensitivity analysis

✉ Maame Akua Korsah
mkorsah@student.unimelb.edu.au

1 School of Mathematics and Statistics, The University of Melbourne, Melbourne, Australia

2 Department of Microbiology and Immunology, Bio21 Institute and Peter Doherty Institute, The University of Melbourne, Melbourne, Australia

3 Melbourne School of Population and Global Health, The University of Melbourne, Melbourne, Australia

Published online: 18 June 2024

1 Introduction

Malaria remains a global health concern that threatens the lives of many children and adults each year. It has proven to be a persistent problem due to the highly adaptive nature of the *Plasmodium* spp. parasites and the female *Anopheles* mosquito vector (Haldar et al. 2018; Rono et al. 2018). Over the past two decades, substantial headway has been made in reducing the global burden of malaria (WHO 2019; World 2021). These reductions are the result of political commitment, increased funding, and the wide-scale deployment of effective malaria control interventions targeting both the human host and the mosquito vector. However, in recent years progress has stalled and has even reversed in regions with moderate to high transmission. This rebound is particularly concerning for the most prevalent malaria parasite, *Plasmodium falciparum*, which is responsible for the majority of malaria-related deaths globally (Perkins et al. 2011; Ahmad et al. 2023). To make matters worse, the COVID-19 pandemic demonstrated how even short-term disruptions in routine malaria interventions can impede progress in achieving elimination in malaria-endemic countries (Hakizimana et al. 2022; Rogerson et al. 2020).

Current malaria control strategies (or measures) include interventions that target the vector population and antimalarial therapeutic measures that target the human host population. Vector control strategies such as insecticide treated nets (ITNs)/long-lasting insecticidal nets (LLINs) and indoor residual spraying (IRS) with insecticides are key elements of current malaria control programs due to their effectiveness at interrupting transmission by reducing the population size of the mosquito vector (WHO 2021). Despite their historical success, these measures have drawbacks such as limited coverage (i.e., only target indoor transmission), being costly to implement and maintain, and potentially leading to the development of insecticide resistance in mosquitoes (Ojuka et al. 2015; WHO 2018; Gari and Lindtjørn 2018). Therapeutic strategies, including the treatment of symptomatic infections with artemisinin-based combination therapy (ACTs) and targeted chemotherapy programs (e.g., intermittent preventive treatment (IPT) and seasonal malaria chemoprevention (SMC)) seek to reduce the number of infected human hosts, thereby reducing malaria morbidity and mortality, as well as onward transmission (WHO 2021). Unfortunately, these therapeutic measures have drawbacks like drug resistance and side effects, limiting long-term reliability (Plowe 2022; Lin et al. 2014). Given the limited budget available for malaria control, it becomes essential to optimize the allocation of resources and select interventions that provide the most significant impact. Thus, if malaria is to be eliminated in an endemic area, there is a need to adopt several strategic interventions simultaneously to avert both outdoor and indoor malaria transmission, and to curtail transmissions from the infectious human reservoir (Gari and Lindtjørn 2018). Mathematical modeling can help determine effective malaria interventions by providing valuable insights into complex disease dynamics and guiding decision-makers in the selection and implementation of the most cost-effective intervention strategies.

Mathematical modelling is effective in helping to tackle many epidemiological problems such as identifying disease determinants and controlling disease spread (Grassly and Fraser 2008; Li 2018). Additionally, mathematical modelling has proven useful in the evaluation of malaria control programs and in assessing the transmission dynam-

ics of infectious diseases amidst interventions (Yang et al. 2017; Korsah 2021; Griffin et al. 2010). In the study of malaria transmission, the $S_H E_H I_H R_H - S_M E_M I_M$ model has been used widely as a simple yet practical approach to understanding the transmission patterns of malaria (and other vector-host infections), adding significantly to our knowledge of malaria (Yang and Ferreira 2000; Ngwa and Shu 2000; Chitnis et al. 2006; Turner et al. 2015; Shah and Gupta 2013; Mojeeb et al. 2017; Baihaqi and Adi-Kusumo 2020). For instance, Chitnis et al. and Osman et al. employed the $S_H E_H I_H R_H - S_M E_M I_M$ model to examine the transmission dynamics of malaria in a human population (Chitnis et al. 2006; Mojeeb et al. 2017; Chitnis et al. 2008). They found that the rate of infection parameters in both humans and mosquitoes are the most influential parameters on the basic reproduction number, $\mathcal{R}_0$ (Mojeeb et al. 2017; Chitnis et al. 2008). Following the results obtained, the authors recommended reducing malaria prevalence with antimalarial treatment and reducing contact rates with IRS and ITNs/LLINs. Osman et al. also emphasised the importance of future research focusing on assessing the impact of interventions and conducting disease control analysis with the $S_H E_H I_H R_H - S_M E_M I_M$ model and to date, a notable research gap remains in this space (Mojeeb et al. 2017).

In this paper, we employ an extension of the $S_H E_H I_H R_H - S_M E_M I_M$ model to consider the impact of interventions targeting the vector, such as IRS and ITNs/LLINs on the spread of malaria, specifically focusing on the transmission of *P. falciparum*, while factoring into the model the transmission characteristics of partial immune individuals. These are individuals who have acquired some level of protection after repeated exposure to malaria parasites but have not developed full immunity that would completely prevent infection. We assume that when these partially immune individuals become infected, they remain asymptomatic but can still transmit the malaria parasite, thus contributing to the continued transmission of malaria. This paper is structured as follows; in Sect. 2, a deterministic transmission model with separate transmission routes for non-immune and partially immune individuals is constructed. We formulate the basic reproduction number of the model and conduct a sensitivity analysis on the model parameters in Sects. 3.1 and 3.2. In Sect. 4, we assess the impact of intervention strategies or measures on malaria transmission. Finally, we provide recommendations for improving malaria control programs, based on our results and discuss the implications of our findings in Sect. 5.

2 Model Formulation

Building on the disease transmission models of Yang et al. and Osman et al., we develop a malaria transmission model that takes into account transmission from both partial and non-immune infectious humans (Yang et al. 2017; Mojeeb et al. 2017). We extend the $S_H E_H I_H R_H - S_M E_M I_M$ model by splitting the susceptible and exposed human classes into two sub-classes each as similarly done by ul Rehman et al. (2022), to capture the transmission properties of both non-immune and partially immune individuals. The human population therefore has six compartments, see Fig. 1;

- S_{H1}: non-immune, uninfected individuals susceptible to symptomatic infection,

- S_{H2}: partially immune, uninfected individuals, susceptible to re-infection (asymptomatic),
- E_{H1}: non-immune individuals in latent phase of symptomatic infection,
- E_{H2}: partially immune individuals in latent phase of asymptomatic infection,
- I_H: symptomatic infectious individuals,
- A_H: asymptomatic infectious individuals.

We divide the mosquito population into (S_M) susceptible, (E_M) exposed and (I_M) infected mosquitoes.

We consider the impact of intervention strategies to provide valuable insights and evidence that can guide decision-making in reducing malaria transmission (Yang et al. 2017; Korsah 2021). We define intervention programs or strategies as measures that aim to lower the prevalence of malaria in an endemic region. To optimize the level of intervention programs needed for the elimination of malaria, we explore the effect of intervention programs (P) on the transmission of malaria. See Fig. 1 for a schematic of the model structure. In the model formulation, we incorporate a constant influx of interventions with rate η. The influx of interventions is also influenced by the number of symptomatic infectious cases (I_H) at a rate of ξ and the interventions decrease at rate κ. Thus the influx rate parameter η can be interpreted as the total uptake rate of intervention measures that decrease the mosquito bite rate without considering the impact of changes in malaria prevalence, whereas the parameter ξ accounts for the influence of symptomatic infectious cases on the influx rate of intervention measures. We assume that the availability and usage of intervention programs, P, affect disease trends by modulating the transmission rate.

The model in Fig. 1, governed by the system of ODEs in Equation (1), can be used to assess the intervention programs necessary for the elimination of malaria in a geographic setting:

$$\frac{dS_{H1}}{dt} = \Lambda_H - \beta_H(P)S_{H1}I_M - \mu_H S_{H1} + \sigma_1 S_{H2}, \tag{1a}$$

$$\frac{dS_{H2}}{dt} = \tau I_H + \sigma_2 A_H - \beta_H(P)S_{H2}I_M - (\mu_H + \sigma_1)S_{H2}, \tag{1b}$$

$$\frac{dE_{H1}}{dt} = \beta_H(P)S_{H1}I_M - (\mu_H + \theta_I)E_{H1}, \tag{1c}$$

$$\frac{dE_{H2}}{dt} = \beta_H(P)S_{H2}I_M - (\mu_H + \theta_A)E_{H2}, \tag{1d}$$

$$\frac{dI_H}{dt} = \theta_I E_{H1} - (\tau + \nu + \mu_H + \gamma)I_H, \tag{1e}$$

$$\frac{dA_H}{dt} = \gamma I_H + \theta_A E_{H2} - (\mu_H + \sigma_2)A_H, \tag{1f}$$

$$\frac{dS_M}{dt} = \Lambda_M - \beta_M(P)S_M(I_H + \chi A_H) - \mu_M S_M, \tag{1g}$$

$$\frac{dE_M}{dt} = \beta_M(P)S_M(I_H + \chi A_H) - (\mu_M + \omega)E_M, \tag{1h}$$

$$\frac{dI_M}{dt} = \omega E_M - \mu_M I_M, \tag{1i}$$

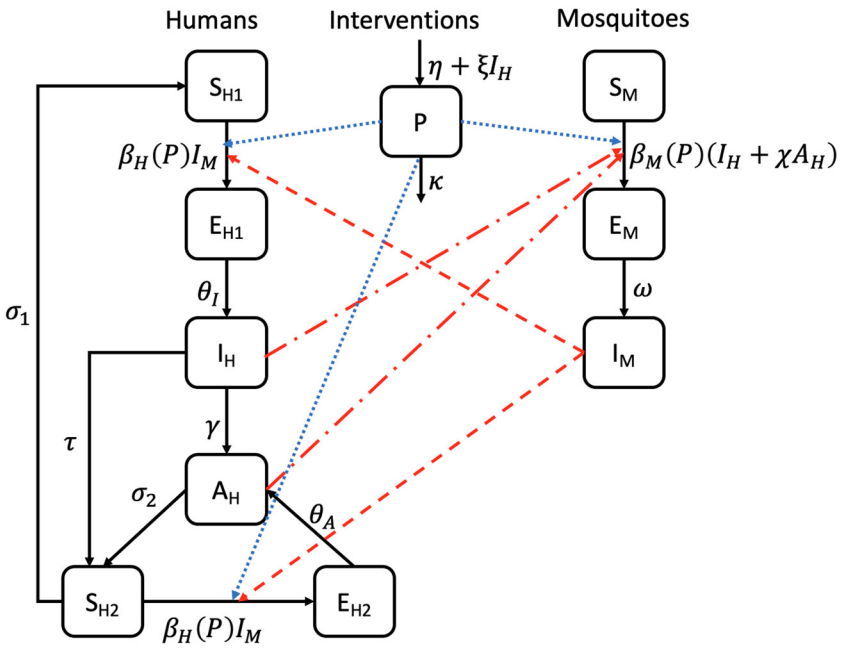


Fig. 1 A compartmental diagram of the host-vector model. The red dash-dotted lines represent transmission from infectious humans to susceptible mosquitoes, the red dashed lines represent transmission from infectious mosquitoes to susceptible humans and the blue dotted lines symbolise the effect of intervention strategies on the transmission of malaria in both host and vector populations. Birth and death rates are not presented in this figure, though they are accounted for in the model. Refer to Table 1 for the definitions of the parameters of the model (Color figure online)

$$\frac{dP}{dt} = \eta + \xi I_H - \kappa P. \tag{1j}$$

The model formulated in Equation (1) describes how susceptible individuals in S_{H1} have a population influx rate of Λ_H and are exposed to *P. falciparum* parasites by an infectious adult female mosquito during blood meals with a frequency-dependent transmission rate of $\beta_H(P)$, moving individuals from S_{H1} into E_{H1}. After a latent phase in E_{H1}, individuals move into the symptomatic infectious class (I_H) where they either self-recover at rate γ and move into the asymptomatic class (A_H) or they are medically treated at rate τ with prescribed drugs such as ACTs (WHO 2021; Trampuz et al. 2003), and move into the S_{H2} compartment. The partially immune yet susceptible individuals in the S_{H2} compartment consist of treated individuals from the I_H class with noninfectious levels of the *Plasmodium* parasites due to treatments received, and asymptomatic persons with infection-induced immunity who transition into this class from the A_H class at rate σ_2. Individuals here can either move back into S_{H1} by the loss of immunity at rate σ_1 or move into E_{H2} by being re-exposed to *P. falciparum* parasites. From E_{H2} individuals become infectious with asymptomatic malaria (A_H) at rate θ_A. The model takes into account the human natural death rate in each class as μ_H as well as mortality due to clinical infection at rate ν.

In the mosquito population, susceptible mosquitoes are exposed to the malaria parasites at a frequency-dependent transmission rate of $\beta_M(P)$ via transmission from both symptomatic and asymptomatic infectious humans and exposed mosquitoes become infectious at rate ω. Transmissions from asymptomatic infectious humans are scaled by a factor, χ, such that $\chi \in [0, 1)$ since asymptomatic humans infect mosquitoes at a lower rate than symptomatic infectious humans (Jiram et al. 2019; Alves et al. 2005; Waltmann et al. 2015).

The intervention class of the model, P, affects the transmission rate functions of the model. Thus, interventions considered here can capture the impact of vector control strategies (IRS and ITNs/LLINs), intermittent preventive treatment (IPTs) with antimalarials, individual measures (environmental preventive measures) such as clearing mosquito breeding sites and/or reducing exposure to mosquitoes (e.g., personal repellents, insect coils and room sprays), and other approaches that can interfere with malaria transmission (Castro et al. 2009; Agyemang-Badu et al. 2023). The intervention class modelled here does not consider other malaria therapeutic measures like ACTs as they affect other aspects of the model.

We further assume that:

(H1) All parameters are non-negative.

(H2) The frequency-dependent transmission rate functions are defined as decreasing functions of the intervention programs P;

$$\beta_H(P) = \frac{\delta}{N_H}\frac{\psi_H}{bP+1}, \qquad \beta_M(P) = \frac{\delta}{N_H}\frac{\psi_M}{cP+1},$$

where b and c are positive-valued constants, N_H is the total human population, $(N_H = S_{H1}+S_{H2}+E_{H1}+E_{H2}+I_H+A_H)$, δ is the biting rate, and ψ_H and ψ_M are the infection success probabilities in humans and mosquitoes respectively.

(H3) The transmission rate functions are decreasing functions of P (i.e. $\beta_*'(P) < 0$) and P takes values in $[0, P_{max}]$ where

$$P_{max} = \frac{\eta + \xi\frac{\Lambda_H}{\mu_H}}{\kappa}.$$

3 Model Analysis

3.1 Formulation of Basic Reproduction Number, $\mathcal{R}_c$

To better understand the proposed framework, we evaluate the basic reproduction number which quantifies new cases generated near the disease-free equilibrium (DFE). The basic reproduction number is formulated using the next generation method established by Diekmann et al., and Van den Driessche and Watmough (Tumwiine et al. 2008; Diekmann et al. 1990; Van den Driessche and Watmough 2002). Refer to Appendix A for the detailed derivation of the basic reproduction number of the model.

The basic reproduction number of the model can be formulated as,

$$\mathcal{R}_c = \sqrt{K_1 + K_2}, \tag{2}$$

where

$$K_1 = \frac{\beta_H(\frac{\eta}{\kappa})\frac{\Lambda_H}{\mu_H}\beta_M(\frac{\eta}{\kappa})\frac{\Lambda_M}{\mu_M}\theta_I\omega}{\mu_M(\mu_M+\omega)(\mu_H+\theta_I)(\tau+\nu+\mu_H+\gamma)}, \tag{3}$$

$$K_2 = \frac{\chi\beta_M(\frac{\eta}{\kappa})\frac{\Lambda_M}{\mu_M}\beta_H(\frac{\eta}{\kappa})\frac{\Lambda_H}{\mu_H}\theta_I\gamma\omega}{\mu_M(\mu_M+\omega)(\mu_H+\theta_I)(\tau+\nu+\mu_H+\gamma)(\mu_H+\sigma_2)}. \tag{4}$$

From Equation (2), we identify two transmission links;

- K_1, which represents transmission from individuals in I_H, and
- K_2, which reflects transmission from self-recovered individuals in A_H.

Transmission from infected mosquitoes is accounted for in each transmission pathway. In the absence of intervention programs ($P = 0$), the basic reproduction number becomes:

$$\mathcal{R}_0 = \sqrt{K_1^* + K_2^*}, \tag{5}$$

where

$$K_1^* = \frac{\beta_H(0)\frac{\Lambda_H}{\mu_H}\beta_M(0)\frac{\Lambda_M}{\mu_M}\theta_I\omega}{\mu_M(\mu_M+\omega)(\mu_H+\theta_I)(\tau+\nu+\mu_H+\gamma)}, \tag{6}$$

$$K_2^* = \frac{\chi\beta_M(0)\frac{\Lambda_M}{\mu_M}\beta_H(0)\frac{\Lambda_H}{\mu_H}\theta_I\gamma\omega}{\mu_M(\mu_M+\omega)(\mu_H+\theta_I)(\tau+\nu+\mu_H+\gamma)(\mu_H+\sigma_2)}. \tag{7}$$

Thus,

$$\mathcal{R}_c \leq \mathcal{R}_0, \tag{8}$$

since the transmission rate functions are decreasing functions of P, reflecting the impact of intervention programs to reduce the spread of malaria.
We note that $\mathcal{R}_c$ does not account for transmission from re-infections, since there are no individuals with partial immunity at the DFE. Thus compartments relating to partial immunity do not influence the calculation of $\mathcal{R}_c$. Refer to Appendix Section A.1 for the conditions for each compartment at the DFE.

Table 1 Definition of the model parameters

Parameter	Description	Baseline values	References
Λ_H	influx rate of susceptible humans	0.235 persons/day	Wu and Hu (2021)
Λ_M	influx rate of susceptible mosquitoes	26.7 mosquitoes/day	Wu and Hu (2021)
δ	mosquito biting rate	1/ day	Wu and Hu (2021)
ψ_H	probability of transmission from infectious mosquito to susceptible human during bite	0.22	Woldegerima et al. (2021); Wu and Hu (2021)
ψ_M	probability of transmission from infectious human to susceptible mosquito during bite	0.24	Woldegerima et al. (2021); Wu and Hu (2021)
μ_H	natural death rate of humans	4.5×10^{-5} /day	Woldegerima et al. (2021); Wu and Hu (2021)
μ_M	natural death rate of mosquitoes	0.0477 /day	Woldegerima et al. (2021); Wu and Hu (2021)
τ	treatment rate of symptomatic infectious humans	0.08 /day	Wu and Hu (2021)
ω	latency rate in mosquitoes	1/9 /day	Center (2020); Stopard et al. (2021)
γ	average untreated symptomatic infection duration rate in humans	0.08 /day	Woldegerima et al. (2021); Wu and Hu (2021)
ν	disease induced mortality rate of humans	0.08 /day	Woldegerima et al. (2021); Wu and Hu (2021)
χ	relative infectiousness of asymptomatic humans	0.8	–
η	influx rate of intervention programs	0.3/day	–
κ	decay rate of intervention programs	0.04/day	–
ξ	growth rate of programs stimulated by symptomatic infections	0.0025/day	–
b	constant coefficient of P in the human transmission rate function	0.5	–
c	constant coefficient of P in the vector transmission rate function	0.4	–
θ_I	latency rate in non-immune humans	1/15 /day	Trampuz et al. (2003)
θ_A	latency rate in partially immune humans	1/20 /day	Wu and Hu (2021)
σ_1	immunity waning rate of partially immune humans	0.01 /day	Woldegerima et al. (2021); Wu and Hu (2021)
σ_2	recovery rate from asymptomatic infectiousness	0.01 /day	Woldegerima et al. (2021); Wu and Hu (2021)

Table 2 Sensitivity index of the model parameters on $\mathcal{R}_c$ and $\mathcal{R}_0$

Parameters	Sensitivity index on $\mathcal{R}_c$ and $\mathcal{R}_0$
δ	1
ψ_H	0.5
ψ_M	0.5
Λ_M	0.5
ω	$\frac{\mu_M}{2(\mu_M+\omega)} > 0$
χ	$\frac{\chi\gamma}{2(1+\chi\gamma)} > 0$
θ_I	$\frac{\mu_H}{2(\mu_H+\theta_I)} > 0$
γ	$\frac{\gamma[\chi(\tau+\nu+\mu_H)-1]}{2(\tau+\nu+\mu_H+\gamma)(1+\chi\gamma)} > 0$
μ_M	$-\frac{3\mu_M+2\omega}{2(\mu_M+\omega)} < 0$
τ	$-\frac{\tau}{2(\tau+\nu+\mu_H+\gamma)} < 0$
ν	$-\frac{\nu}{2(\tau+\nu+\mu_H+\gamma)} < 0$
σ_2	$-\frac{\sigma_2}{2(1+\mu_H+\sigma_2)} < 0$
Interventional Parameters	Sensitivity index on $\mathcal{R}_c$
κ	$\frac{\eta[2bc\eta+(b+c)\kappa]}{2(b\eta+\kappa)(c\eta+\kappa)} > 0$
b	$-\frac{b\eta}{2(b\eta+\kappa)} < 0$
c	$-\frac{c\eta}{2(c\eta+\kappa)} < 0$
η	$-\frac{\eta[2bc\eta+(b+c)\kappa]}{2(b\eta+\kappa)(c\eta+\kappa)} < 0$

3.2 Sensitivity Analysis on $\mathcal{R}_c$

We conduct a sensitivity analysis on $\mathcal{R}_c$ to obtain qualitative information on how the model parameters affect $\mathcal{R}_c$ by employing the normalized forward index, ζ of $\mathcal{R}_c$ for a parameter k, (Rodrigues et al. 2013) as

$$\zeta_k^{\mathcal{R}_c} = \frac{\partial \mathcal{R}_c}{\partial k} \cdot \frac{k}{\mathcal{R}_c}.$$

We compare the sensitivity index of the parameters on $\mathcal{R}_c$ and $\mathcal{R}_0$ in Equations (2) and (5), and observe that the normalised forward index, ζ of both $\mathcal{R}_c$ and $\mathcal{R}_0$ is the same for all parameters except for b, c, η and κ, which are parameter related to the interventions class P as $\mathcal{R}_0$ is formulated in the absence of intervention strategies. The results obtained are presented in Table 2.

Based on Table 2, we deduce that parameters such as the mosquito biting rate (δ), infection success probabilities (ψ_H, ψ_M) and decay rate of intervention programs (κ), which have positive indices contribute to the initial spread of malaria (in that as the parameter increases, $\mathcal{R}_c$ increases). In contrast the treatment rate of infected persons (τ), interventions recruitment/funding rate (η), and mosquito death rate (μ_M) parameters with negative indices reduce $\mathcal{R}_c$. Some model parameters are not included

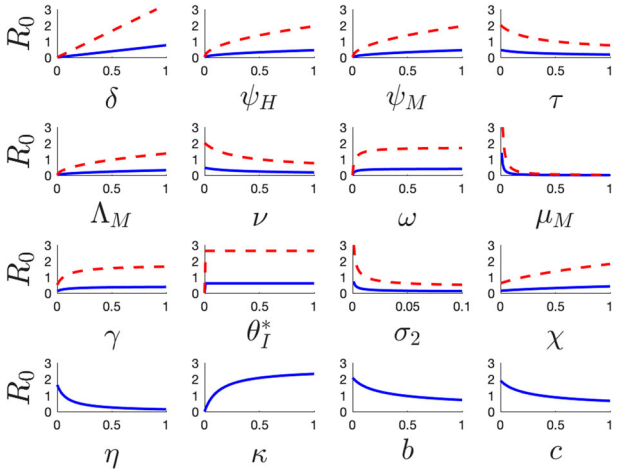


Fig. 2 Plots from a local sensitivity (see Equations (2) and (5)) analysis conducted on the model. In these plots, the blue solid lines illustrate the variations in $\mathcal{R}_c$, as individual parameters change, whereas the red dashed curves illustrate the variations in $\mathcal{R}_0$ with respect to the specific parameter being analyzed, with all other parameters maintained at their baseline values as detailed in Table 1 (Color figure online)

in Table 2, such as σ_1, θ_A, and ξ, since they do not exert a direct influence on $\mathcal{R}_c$, see Equation (2). Note that we exclude the human birth and death rates from the $\mathcal{R}_c$ sensitivity analysis, as these factors are not directly adjustable in the context of malaria control strategies. The focus is on parameters that are amenable to intervention, which is more pertinent for policy considerations.

4 Numerical Results

4.1 Local Sensitivity Analysis on $\mathcal{R}_c$

We substantiate the parameter sensitivity results in Table 2 by plotting $\mathcal{R}_c$ and $\mathcal{R}_0$ as a function of individual parameters in Fig. 2. As expected, parameters with positive indices exhibit a positive impact on both $\mathcal{R}_c$ and $\mathcal{R}_0$, while conversely, parameters with negative indices have a negative effect. The difference in impact between $\mathcal{R}_c$ and $\mathcal{R}_0$ is clear from Fig. 2, and indicates that the absence of intervention programs leads to an increase in the basic reproduction number, which supports the findings from Equation (8).

4.2 Impact of Variation in Interventions on Malaria

In Fig. 3, we present the outcomes of a sensitivity analysis to investigate the combined effect of changes in η and κ on $\mathcal{R}_c$. We observe that the intervention decay rate, κ, has an increasing effect on $\mathcal{R}_c$ whereas the recruitment rate of interventions, η, has an

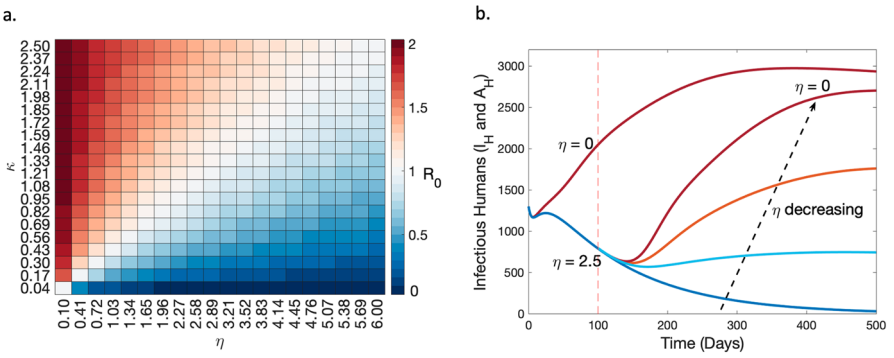


Fig. 3 **a.** A sensitivity analysis of $\mathcal{R}_c$ on the intervention parameters κ and η. The colour bar represents $\mathcal{R}_c$ values ranging from 0 (blue) indicating a negative growth of the disease to 2 (red) indicating a positive initial disease growth. The subplot **a.** is derived from the solution to Equation (2). **b.** Simulation results comparing the dynamics of infectious human cases from a steady declining situation (dark blue line), as the recruitment rate of intervention programs is decreased at 100 days compared to having $\eta = 0$ from the start. Four decreasing scenarios of η are considered at 100 days from $\eta = 2.5$ (dark blue line) to $\eta = 0$ (dark red line) with $\kappa = 0.17$ in all scenarios. Results in subplot **b.** are obtained by solving Equation (1) and recording changes in Equations (1e) and (1f) as η varies. In generating **b.** the initial condition was set at $S_{H1}(0) = 2400$, $S_{H2}(0) = 1000$, $E_{H1}(0) = 600$, $E_{H2}(0) = 400$, $I_H(0) = 900$, $A_H(0) = 400$, $S_M(0) = 1500$, $E_M(0) = 200$, $I_M(0) = 150$, $P(0) = 1$ (Color figure online)

inhibitory effect on $\mathcal{R}_c$ which is consistent with $\mathcal{R}_c$ decreasing as interventions (P) increases.

From Fig. 3a, we have identified the level of recruitment and decay of intervention measures necessary to prevent malaria outbreaks given the dynamics of transmission in an endemic setting (e.g. that push $\mathcal{R}_c < 1$). The white region of Fig. 3a represents the level required to control initial malaria transmission, where $\mathcal{R}_c$ drops to 1. The blue region represents the region of the parameter space where malaria is suppressed but achieves a more substantial reduction in $\mathcal{R}_c$ than necessary to suppress outbreaks. We also perform numerical simulations of the model to investigate how variations in intervention strategies resulting from decreasing intervention funds and the discontinuation of established strategies affects the number of infectious cases in the human population before and after disease elimination. Here we classify infectious cases, I, as the sum of symptomatic and asymptomatic infectious humans, that is, $I = I_H + A_H$. We consider a situation where a diminishing trend in malaria cases results in reduced funds for antimalarial interventions (Diptyanusa and Zablon 2020; Weiss et al. 2021). This behaviour of funding agencies is factored into the model by reducing the recruitment rate of interventions, η. It is important to clarify that the concept of funding in this context represents the influx into P, rather than a specific dollar value. Figure 3b presents the simulation results of the number of infectious humans under different varying scenarios of η. We observe that as funding for malaria elimination programs decreases, infectious cases increase. This result was generated under the assumption that when there is a 40% decrease in infectious cases, stakeholders will consider decreasing funding rates. The scenario where $\eta = 0$ after the initial disease decline, leads to a higher increase in infectious cases, closer to the "no

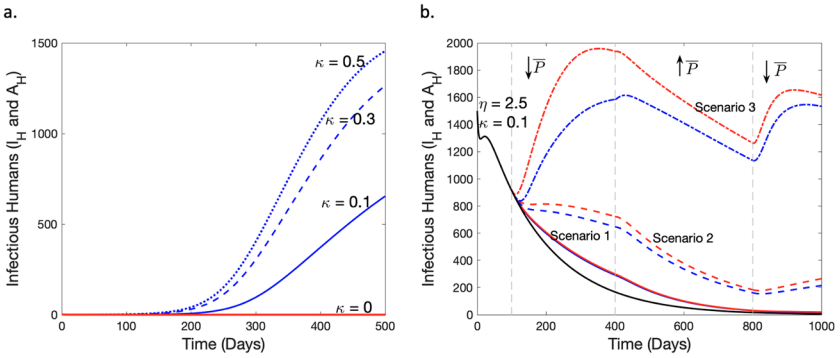


Fig. 4 Simulation results exploring how variations in interventions affect infectious trends. **a.** After-elimination scenarios on how the management (decay) of intervention strategies can affect infectious human cases in the first 500 days post-elimination. After elimination, we set $\eta = 0$ and consider four scenarios of κ; $\kappa = 0$ (red solid line), $\kappa = 0.1$ (blue solid line), $\kappa = 0.3$ (blue dashed line) and $\kappa = 0.5$ (blue dotted line). **b.** The impact of time-varying intervention strategies on malaria-infectious human cases. The solid black line represents the ideal (baseline) scenario with a constant supply and decay rate of interventions ($\eta = 2.5$ and $\kappa = 0.1$), the blue line represents results from variations in the recruitment rate of intervention strategies, η, while the red lines represent simulation results from a corresponding change in the decay rate of interventions, κ. The changes are chosen such that $\overline{P}$, (i.e. P at the DFE) for each change in η and κ is equal. We consider three scenarios of unsteady intervention strategies from day 100 and explore further variations in the supply and decay rate of interventions from days 400 and 800. These days are marked by the vertical grey dashed lines. Scenario 1 is marked by the solid red and blue lines, Scenario 2 by the dashed lines, and Scenario 3 by the dash-dotted lines (specific details are discussed in the main text). Solution of both subplots **a.** and **b.** are obtained by solving the model system in Equation (1) and recording the specific changes in Equations (1e) and (1f) (Color figure online)

control" situation with $\eta = 0$ from the start. In fact, this scenario with $\eta = 0$ after the initial decline will ultimately hit the same steady state as the "no control" situation. However, maintaining $\eta = 2.5$ sees malaria approach elimination. Thus we can infer from the results of Fig. 3b that in order to sustain a diminishing trend in infectious malaria cases, it is likely necessary to either raise or maintain the funding rates for intervention recruitment strategies.

To explore the post-elimination prospects of malaria in endemic regions, we conducted numerical experiments using the baseline parameter values in Table 1, setting $\delta = 3$, $\psi_H = 0.5$, and $\psi_M = 0.5$, until the time point where the number of infectious individuals, denoted as I, falls below a specified threshold ϵ. Using the same parameter values and compartmental dynamics observed at that particular point in time (i.e. we set $I_H(0) = I_H(\text{at elimination}) + 1$ and maintained the values of all other compartments), we then introduced a single symptomatic infectious human and varied the decay rate of the intervention strategies, κ (as per Fig. 4a). In reality, malaria elimination is when $I = 0$, however in practice we set malaria elimination status at a threshold of $\epsilon = 0.3 > 0$ since we are employing a continuum model. By varying the value of κ in Fig. 4a, we observe an increase in infectious cases as the decay rates of interventions increases. We thus infer that the discontinuation of intervention programs after elimination could lead to a reemergence of malaria. Setting $\kappa = 0$, however, results in an unperturbed malaria elimination state even with the introduction of an infectious case as strategies

to control the spread of malaria are still available. Our results suggest that maintenance of established intervention strategies is, therefore, necessary to maintain elimination status.

In light of the current erratic trends in malaria cases globally, we investigate the dynamics of infectious cases resulting from a changing supply of funds for malaria intervention programs and the temperamental utilization of interventions by exploring variations in η ($\Delta\eta$) and κ ($\Delta\kappa$) such that $\overline{P}$, the P at the DFE, for each change in η and κ is equal (i.e. $\overline{P}_{\Delta}\eta = \overline{P}_{\Delta}\kappa$, where $\overline{P} = \frac{\eta}{\kappa}$). In each scenario, a percentage change in $\overline{P}$ is achieved via a modification of the parameter η or κ. From Fig. 4b, we observe three scenarios (specific details below) of trends in malaria cases resulting from an initial decrease in $\overline{P}$ after the baseline scenario at day 100. This is followed by a substantial increase in $\overline{P}$ from day 400, aimed at rectifying possible increasing trends of infectious cases. Finally, $\overline{P}$ is decreased after day 800 by a percentage less than the initial decrease at day 100. This is done to incorporate positive but deficient human behaviour targeted towards malaria elimination into our investigation of the unsteady trends in malaria cases. We discuss the details of variations considered in all three scenarios below.

- Scenario 1 (solid lines in red and blue) – After 100 days of the baseline simulation, we decreased $\overline{P}$ by 30% ($\eta = 1.75$ in blue or $\kappa = 0.1429$ in red) and observed similar results for the variations in both κ (red) and η (blue), that is a general reduction in malaria cases. After day 400, we increase $\overline{P}$ by 50% ($\eta = 2.625$ in blue or $\kappa = 0.0953$ in red) and observe human infectious cases fall closer to elimination levels. With the number of infectious cases nearing elimination, a subsequent 20% decrease in $\overline{P}$ ($\eta = 2.1$ in blue or $\kappa = 0.1191$ in red) at day 800 results in further declines as the infectious cases present are not enough to cause a rise in cases.
- Scenario 2 (dashed lines in red and blue) – After day 100, we decrease $\overline{P}$ by 55% ($\eta = 1.125$ in blue or $\kappa = 0.2222$ in red) which results in a higher increase in cases for the corresponding change in κ (red) than in η (blue) by day 400. We then increase $\overline{P}$ by 75% ($\eta = 1.9688$ in blue or $\kappa = 0.127$ in red) and observe a similar reduction trend in both η and κ from day 400 to 800. We finally reduce $\overline{P}$ by 35% ($\eta = 1.2797$ in blue or $\kappa = 0.1954$ in red) after day 800 to observe an increase in both at day 1000.
- Scenario 3 (dash-dotted lines in red and blue) – $\overline{P}$ is cut by 80% ($\eta = 0.5$ in blue or $\kappa = 0.5$ in red) after day 100 which leads to a substantial rise in malaria cases by day 400. We continue by increasing $\overline{P}$ by 90% ($\eta = 0.95$ in blue or $\kappa = 0.2632$ in red) and observe a sharp decline in malaria cases for the change in η (blue) compared to κ (red) by day 800. We finally cut $\overline{P}$ by 50% ($\eta = 0.475$ in blue or $\kappa = 0.5264$ in red) after day 800 and observe a climb in cases.

In all three scenarios presented in Fig. 4b, we show that while the inconsistent supply of funds for intervention strategies (results for changing η in blue) has a notable impact on infectious cases, the unsteady maintenance of interventions (results for changing κ in red) has a more pronounced impact on infection trends.

4.3 IRS, LLINs and Individual Interventions Scenarios

We conduct a scenario study to investigate how IRS, LLINs, and individual (preventive) measures such as clearing mosquito breeding sites and reducing mosquito exposure (Castro et al. 2009; Agyemang-Badu et al. 2023) in the presence of high and low levels of risk aversion in the community, affect the patterns of symptomatic malaria infections. To this effect, the model parameters, η, κ, ξ, b and c, which are associated with the intervention class were adjusted to reflect the effectiveness of the selected interventions. Drawing from existing literature, we incorporate into our scenario analysis the intervention's implementation, durability and efficacy. Notably, LLINs exhibit an efficacy rate of approximately 77% among individuals using it, decreasing malaria prevalence by about 77%, and have a lifespan of three years (Wubishet et al. 2021; Tan et al. 2016; Kilian et al. 2021; Musa et al. 2020). Based on this information, we set b and c at 0.8 to mimic a high efficacy rate of LLINs. Note that b and c are the constant coefficients of P in the human and vector transmission rate functions respectively, modelled to capture the effect of intervention strategies on the transmission rate functions. In the LLINs scenario, we assume a baseline daily rate of flux into P of 0.5 with its usage growing at a rate of 0.08/day/symptomatic case as stimulated by the number of symptomatic cases (see LLINs column of Table 3). In the study, we also examine how the extent of LLINs usage (and the duration of IRS coverage) can influence symptomatic infections. Since the duration of LLINs exceeds the timeline of this study (a year), we model the κ values of LLINs to majorly capture the extent of LLINs usage. We assume a 90% usage to represent a high level of usage of bed nets and 40% percent as low usage. This percentage difference was factored into the choice of κ values so that the ratio of $\overline{P}$ for high usage to $\overline{P}$ for low usage is 9:4 (refer to LLINs column of Table 3 ($\overline{P} = \frac{\eta}{\kappa}$)). IRS, on the other hand, demonstrates high varying efficacy depending on coverage levels, and a duration ranging from 5 to 8 months contingent upon the specific chemical employed (Chitnis et al. 2010; Worrall et al. 2007; Sherrard-Smith et al. 2018; Dengela et al. 2018; Rehman et al. 2011; Fongnikin et al. 2020). In the IRS scenario, we assume a high coverage spraying is done at the start of the study that on average, decays in 5 months for the short duration case and 8 months for the long duration case. These durations were considered in the values chosen for the parameter κ found in the IRS column of Table 3. The parameters b and c we set at 0.85 to depict a high efficacy rate while η and ξ were set to 0 in line with the assumption that IRS intervention will not be administered again for the period of 1 year considered. Conversely, we assume relatively lower efficiency and durability for the localized individual interventions and compare the impact of the individual interventions in the presence of high ($\xi = 0.005$) and low ($\xi = 0.001$) levels of intervention growth rate stimulated by the number of symptomatic infectious cases, see Individual Measures column of Table 3. However, we consider a higher usage of these individual measures when infectious cases are on the rise, acknowledging the adaptable nature of human behavior in response to changing disease dynamics (Castro et al. 2009). Assuming a yearly recurrent implementation of these interventions, we run simulations for 365 days to assess and compare the effects of these three strategies against the baseline scenario, where no interventions are employed. In the baseline

Table 3 Intervention parameter values utilised for the simulation results in Fig. 5

Parameters	No Interventions	Individual Measures		IRS		LLINs	
		Low ξ	High ξ	Long Duration	Short Duration	High usage	Low usage
η	0/day	0.005/day	0.005/day	0/day	0/day	0.5/day	0.5/day
ξ	0/day	0.001/day	0.005/day	0/day	0/day	0.08/day	0.08/day
κ	0/day	0.15/day	0.15/day	0.018/day	0.03/day	0.2/day	0.45/day
b & c	0	0.4	0.4	0.85	0.85	0.8	0.8

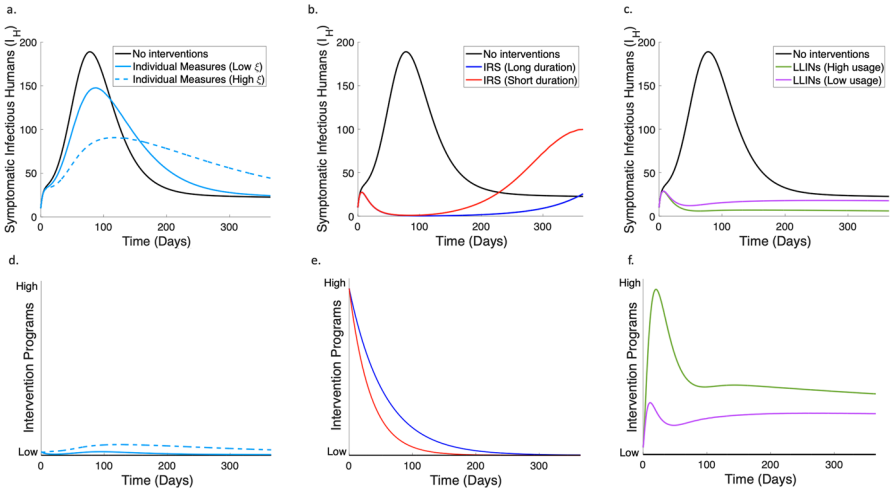


Fig. 5 Simulation results capturing the impact of IRS, LLINs, and individual preventive measures on symptomatic infectious humans over a period of 365 days. **a.** Results comparing the impacts of individual measures on symptomatic malaria cases with the baseline when no interventions are implemented. **b.** Results comparing the impacts of IRS (long and short duration) with the baseline of no intervention measures on symptomatic infectious cases. **c.** Results comparing the impacts of LLINs (high and low usage) with no interventions on symptomatic infectious cases. **d.–f.** Graphical representation of the levels of interventions considered in the simulation studies in **a.–c.** respectively (color figure online)

scenario, we assume that no intervention measures are active during the entire study period, and we set all related parameters to zero (see No Interventions column of Table 3). In Fig. 5, we present a summary of the results of this study and provide the intervention parameter values utilised in the simulation study in Table 3.

Fig. 5 captures the impact of IRS, LLINs and individual measures on symptomatic infectious humans. In Figs. 5a. and 5d. we observe that individual preventive measures that exhibit a relatively low impact amongst the three scenarios, can reduce symptomatic infections during the period of heightened disease activity. We observe a greater reduction in symptomatic infectious cases during this period with a high-risk aversion rate (ξ) level than with a low rate. Moreover, in an extended timeframe, beyond 365 days, we observe a declining trend in cases when using these individual measures, which falls below the baseline scenario. In Figs. 5b. and 5e., our observations indicate that implementation of IRS leads to a significant reduction in malaria infection cases, within its designated effective duration. After IRS efficacy wanes there is an upsurge in the number of infectious cases. Specifically, within the 365 day period the 5-month IRS scenario has a peak prevalance lower than the peak of the baseline scenario, while in the 8-month IRS scenario has an even lower peak. In Figs. 5c. and 5f., high usage of LLINs has greater impact on symptomatic infectious cases. Conversely, the scenario involving low LLINs usage initially demonstrates a decline in the first 50 days. However, as the number of cases reduces, the utilization of bed nets decreases further, leading to a resurgence in cases approaching the baseline scenario, as observed in Figs. 5c. and f.

Taking into account all the interventions considered in the scenario study, our results suggest that the extensive utilization of LLINs and IRS within their designated effective durations has the potential to curb endemic malaria trends effectively. Nonetheless, when LLINs, IRS, and other highly effective interventions are unavailable, our modelling reveals that implementing individual preventive measures is better than adopting no interventions in the long run.

5 Discussion

In this paper, an extension of the $SEIR - SEI$ host-vector model is employed to study the impact of malaria intervention programs. Our work is targeted towards understanding the current trends of malaria cases in response to malaria interventions as well as assessing the interventions necessary for malaria control and elimination. The extended model is analysed to formulate the basic reproduction number, consistent with previous studies (Yang et al. 2017; Yang and Ferreira 2000; Mojeeb et al. 2017; Chitnis 2005; Olaniyi et al. 2020; Obabiyi and Olaniyi 2019). In our assessment of the basic reproduction number of the model, we identified two transmission pathways that can assist decision-making in the prevention of malaria outbreaks, which we termed as K_1 and K_2 (Equation (2)). K_1 represents transmissions from individuals in the symptomatic infectious human class, I_H, whereas K_2 considers transmissions from self-recovered individuals in the asymptomatic infectious human class, A_H. It is worth noting that both pathways, K_1 and K_2 do not consider re-infections in the infectious classes. Thus K_1 transmissions can be reduced by employing vector control strategies, intermittent preventive treatments of malaria in infants, pregnant people, and children, as well as the RTS,S/AS01 (RTS,S) vaccine recommended by the WHO for the prevention of *P. falciparum* malaria in children. K_2 transmissions on the other hand, can be reduced with strategies like mass screening and treatment (MSAT), focal screening and treatment (FSAT), and mass drug administration (MDA) that typically focuses on asymptomatic infections as well as through educative campaigns promoting the clinical treatment of malaria cases with strategies like mass fever treatment (MFT) to reduce the number of symptomatic infections that go untreated (Nguyen 2016; Kim et al. 2021; Casares et al. 2010; WHO 2021).

A sensitivity analysis conducted on the model demonstrates that several parameters such as the mosquito biting rate (δ), infection success rates (ψ_H, ψ_M) and decay rate of intervention programs (κ) are directly proportional to $\mathcal{R}_c$ whereas parameters like the treatment rate of infected persons (τ), interventions recruitment rate (η), and mosquito death rate (μ_M) are inversely proportional to $\mathcal{R}_c$. These results are consistent with the findings of existing literature (Mojeeb et al. 2017; Chitnis 2005; Shretta et al. 2020). Our study on the impact of variations in preventive intervention strategies shows that reducing funds for malaria interventions in response to a decline in the number of malaria cases may result in the resurgence of malaria. These results reflect the current rising trends of malaria cases after the gradual decline in malaria cases from 2017-2019, as funding for malaria intervention programs was reduced in order to support the control of COVID-19 outbreaks (WHO 2022; Hogan et al. 2020; Roberts 2021). Our modeling results highlight the critical importance of maintaining and, when fea-

sible, increasing funding for malaria intervention strategies rather than decreasing it. We found that sustained investment in intervention programs is essential for preserving malaria elimination status. Therefore, regions that have successfully eliminated malaria must prioritize long-term maintenance of malaria strategies, including detecting and treating new infections among migrants, to prevent the re-emergence of cases (Jun et al. 2021; Shretta et al. 2016). Our intervention scenario study demonstrates that implementing IRS with an extended effective duration and promoting the widespread use of LLINs are promising strategies for reducing symptomatic malaria infections. These findings are consistent with previous literature and emphasize the need for continued support for such interventions (Sherrard-Smith et al. 2018; Pryce et al. 2022; Pryce and Lengeler 2018; Enahoro et al. 2020; Accrombessi et al. 2024; Tiedje et al. 2017; Kateera et al. 2015; Okiring et al. 2022; Raghavendra et al. 2017; Gogue et al. 2020; Tapera 2019; Obembe et al. 2014). Additionally, the study illuminates the potential value of individual preventive measures, albeit with a relatively low impact. These measures can complement other interventions or serve as viable options in settings where more potent interventions are unavailable.

Moving forward, an expansion of this work is recommended to calibrate the model to data from a malaria endemic setting while inferring parameters for the interventions used in the setting. Factors such as age structure, seasonality, and migration, which are major determinants of malaria trends in endemic regions, were not factored in the model and could be considered in future extensions. Additionally, the interventions class of the model did not explicitly consider the dynamics of strategies such as RTS,S vaccine roll-out, the use of larvicides, MSAT, and the development of better healthcare systems in endemic areas. A future study based on data from a endemic location where various interventions are introduced and stopped over the course of an epidemic, could be helpful to calibrate intervention-specific parameters. While these limitations may affect the application of results presented in the study, the study provides an overview of the transmission characteristics of a typical endemic area and thus can be adapted to a specific setting by including additional characteristics of that setting into the model. Several concerns remain unresolved in relation to the behavioural trends of the *Plasmodium* parasites such as their heterogeneity and drug resistance which hinder the elimination of malaria. However, the results of this study suggest that the continuous maintenance of established intervention strategies in endemic areas can provide progress towards malaria elimination. While variations in the implementation of interventions may occur due to economic constraints, it is crucial to foster a culture of maintenance for malaria elimination and potential eradication. Our findings indicate that achieving malaria elimination is associated with a high level of utilization and consistent funding of interventions. The work presented in this paper can potentially contribute to developing effective strategies for malaria control and elimination. By identifying key transmission pathways and emphasizing the importance of intervention maintenance, our findings can guide decision-makers and stakeholders in their efforts to combat malaria and improve public health.

A Model Analysis and Simulation Results

A.1 Basic Reproduction Jumber Using the Next Generation Method

We start by finding the new infection matrix:

$$f = \begin{bmatrix} \beta_H(P)S_{H1}I_M \\ \beta_H(P)S_{H2}I_M \\ 0 \\ 0 \\ \beta_M(P)S_M(I_H + \chi A_H) \\ 0 \end{bmatrix} \Rightarrow \mathcal{F} = \begin{bmatrix} \frac{\partial f_1}{\partial E_{H1}} & \frac{\partial f_1}{\partial E_{H2}} & \frac{\partial f_1}{\partial I_H} & \frac{\partial f_1}{\partial A_H} & \frac{\partial f_1}{\partial E_M} & \frac{\partial f_1}{\partial I_M} \\ \frac{\partial f_2}{\partial E_{H1}} & \frac{\partial f_2}{\partial E_{H2}} & \frac{\partial f_2}{\partial I_H} & \frac{\partial f_2}{\partial A_H} & \frac{\partial f_2}{\partial E_M} & \frac{\partial f_2}{\partial I_M} \\ \frac{\partial f_3}{\partial E_{H1}} & \frac{\partial f_3}{\partial E_{H2}} & \frac{\partial f_3}{\partial I_H} & \frac{\partial f_3}{\partial A_H} & \frac{\partial f_3}{\partial E_M} & \frac{\partial f_3}{\partial I_M} \\ \frac{\partial f_4}{\partial E_{H1}} & \frac{\partial f_3}{\partial E_{H2}} & \frac{\partial f_4}{\partial I_H} & \frac{\partial f_4}{\partial A_H} & \frac{\partial f_4}{\partial E_M} & \frac{\partial f_4}{\partial I_M} \\ \frac{\partial f_5}{\partial E_{H1}} & \frac{\partial f_5}{\partial E_{H2}} & \frac{\partial f_5}{\partial I_H} & \frac{\partial f_5}{\partial A_H} & \frac{\partial f_5}{\partial E_M} & \frac{\partial f_5}{\partial I_M} \\ \frac{\partial f_6}{\partial E_{H1}} & \frac{\partial f_6}{\partial E_{H2}} & \frac{\partial f_6}{\partial I_H} & \frac{\partial f_6}{\partial A_H} & \frac{\partial f_6}{\partial E_M} & \frac{\partial f_6}{\partial I_M} \end{bmatrix},$$

which gives

$$\mathcal{F} = \begin{bmatrix} 0 & 0 & 0 & 0 & 0 & \beta_H(P)S_{H1} \\ 0 & 0 & 0 & 0 & 0 & \beta_H(P)S_{H2} \\ 0 & 0 & 0 & 0 & 0 & 0 \\ 0 & 0 & 0 & 0 & 0 & 0 \\ 0 & 0 & \beta_M(P)S_M & \chi\beta_M(P)S_M & 0 & 0 \\ 0 & 0 & 0 & 0 & 0 & 0 \end{bmatrix}.$$

And the transition matrix:

$$v = \begin{bmatrix} (\mu_H + \theta_I)E_{H1} \\ (\mu_H + \theta_A)E_{H2} \\ -\theta_I E_{H1} + (\tau + \nu + \mu_H + \gamma)I_H \\ -\gamma I_H - \theta_A E_{H2} + (\mu_M + \sigma_2)A_H \\ (\mu_M + \omega)E_M \\ -\omega E_M + \mu_M I_M \end{bmatrix} \Rightarrow \mathcal{V} = \begin{bmatrix} \frac{\partial v_1}{\partial E_{H1}} & \frac{\partial v_1}{\partial E_{H2}} & \frac{\partial v_1}{\partial I_H} & \frac{\partial v_1}{\partial A_H} & \frac{\partial v_1}{\partial E_M} & \frac{\partial v_1}{\partial I_M} \\ \frac{\partial v_2}{\partial E_{H1}} & \frac{\partial v_2}{\partial E_{H2}} & \frac{\partial v_2}{\partial I_H} & \frac{\partial v_2}{\partial A_H} & \frac{\partial v_2}{\partial E_M} & \frac{\partial v_2}{\partial I_M} \\ \frac{\partial v_3}{\partial E_{H1}} & \frac{\partial v_3}{\partial E_{H2}} & \frac{\partial v_3}{\partial I_H} & \frac{\partial v_3}{\partial A_H} & \frac{\partial v_3}{\partial E_M} & \frac{\partial v_3}{\partial I_M} \\ \frac{\partial v_4}{\partial E_{H1}} & \frac{\partial v_4}{\partial E_{H2}} & \frac{\partial v_4}{\partial I_H} & \frac{\partial v_4}{\partial A_H} & \frac{\partial v_4}{\partial E_M} & \frac{\partial v_4}{\partial I_M} \\ \frac{\partial v_5}{\partial E_{H1}} & \frac{\partial v_5}{\partial E_{H2}} & \frac{\partial v_5}{\partial I_H} & \frac{\partial v_5}{\partial A_H} & \frac{\partial v_5}{\partial E_M} & \frac{\partial v_5}{\partial I_M} \\ \frac{\partial v_6}{\partial E_{H1}} & \frac{\partial v_6}{\partial E_{H2}} & \frac{\partial v_6}{\partial I_H} & \frac{\partial v_6}{\partial A_H} & \frac{\partial v_6}{\partial E_M} & \frac{\partial v_6}{\partial I_M} \end{bmatrix},$$

which gives

$$\mathcal{V} = \begin{bmatrix} (\mu_H + \theta_I) & 0 & 0 & 0 & 0 & 0 \\ 0 & (\mu_H + \theta_A) & 0 & 0 & 0 & 0 \\ -\theta_I & 0 & (\tau + \nu + \mu_H + \gamma) & 0 & 0 & 0 \\ 0 & -\theta_A & -\gamma & (\mu_H + \sigma_2) & 0 & 0 \\ 0 & 0 & 0 & 0 & (\mu_M + \omega) & 0 \\ 0 & 0 & 0 & 0 & -\omega & \mu_M \end{bmatrix}.$$

We compute $\mathcal{R}_c$ by finding the spectral radius, ρ of the matrix product of $\mathcal{FV}^{-1}$ where

$$\mathcal{FV}^{-1} = \begin{bmatrix} 0 & 0 & 0 & 0 & \frac{\beta_H(P)S_{H1}\omega}{\mu_M(\mu_M+\omega)} & \frac{\beta_H(P)S_{H1}}{\mu_M} \\ 0 & 0 & 0 & 0 & \frac{\beta_H(P)S_{H2}\omega}{\mu_M(\mu_M+\omega)} & \frac{\beta_H(P)S_{H2}}{\mu_M} \\ 0 & 0 & 0 & 0 & & \\ 0 & 0 & 0 & 0 & 0 & 0 \\ m & \frac{\chi\beta_M(P)S_M\theta_A}{(\mu_H+\theta_A)(\mu_H+\sigma_2)} & n & \frac{\chi\beta_M(P)S_M}{(\mu_H+\sigma_2)} & 0 & 0 \\ 0 & 0 & 0 & 0 & 0 & 0 \end{bmatrix}$$

and

$$m = \frac{\beta_M(P)S_M\theta_I(\mu_H+\sigma_2)+\chi\beta_H(P)S_M\theta_I\gamma}{(\tau+\nu+\mu_H+\gamma)(\mu_H+\sigma_2)(\mu_H+\theta_I)},$$
$$n = \frac{\beta_M(P)S_M(\mu_H+\sigma_2)+\chi\beta_H(P)S_M\gamma}{(\tau+\nu+\mu_H+\gamma)(\mu_H+\sigma_2)}.$$

We consider the model at the disease-free equilibrium (DFE), $\mathcal{X}_o = (S_{H1_o}, S_{H2_o}, E_{H1_o}, E_{H2_o}, I_{H_o}, A_{H_o}, S_{M_o}, E_{M_o}, I_{M_o}, P_o) = \left(\frac{\Lambda_H}{\mu_H}, 0, 0, 0, 0, 0, \frac{\Lambda_M}{\mu_M}, 0, 0, \frac{\eta}{\kappa}\right)$.

Note that for the DFE, $\mathcal{X}_o$, $S_{H2_o} = 0$ since S_{H2} represents individuals with partial immunity derived from an earlier infection. We therefore arrive at:

$$\mathcal{R}_c = \rho(\mathcal{FV}^{-1}) = \sqrt{K_1 + K_2}, \tag{9}$$

where K_1 and K_2 are defined as;

$$K_1 = \frac{\beta_H(\frac{\eta}{\kappa})\frac{\Lambda_H}{\mu_H}\beta_M(\frac{\eta}{\kappa})\frac{\Lambda_M}{\mu_M}\theta_I\omega}{\mu_M(\mu_M+\omega)(\mu_H+\theta_I)(\tau+\nu+\mu_H+\gamma)}, \tag{10}$$

$$K_2 = \frac{\chi\beta_M(\frac{\eta}{\kappa})\frac{\Lambda_M}{\mu_M}\beta_H(\frac{\eta}{\kappa})\frac{\Lambda_H}{\mu_H}\theta_I\gamma\omega}{\mu_M(\mu_M+\omega)(\mu_H+\theta_I)(\tau+\nu+\mu_H+\gamma)(\mu_H+\sigma_2)}. \tag{11}$$

A.2 Example Simulation Results of the Model

We provide numerical simulations of the model framework utilizing parameter estimates from previous literature (Trampuz et al. 2003; Wu and Hu 2021; Woldegerima et al. 2021; Center 2020) presented in Table 1 to generate graphical representations of the model dynamics towards the disease-free (DFE) and endemic equilibria (EE). In exploring the model system at the two equilibria, the basic reproduction number, $\mathcal{R}_c$ was set at $\mathcal{R}_c < 1$ and $\mathcal{R}_c > 1$ to depict the DFE and EE behavioural trends. We present the trends of the system in both the host and vector populations.

From our example simulation in Fig. 6a, showing the disease-free equilibrium, it is noticed that the second class of susceptible individuals, S_{H2}, approaches zero like the diseased classes of the human population as $\mathcal{R}_c < 1$. This behaviour is contrary to the

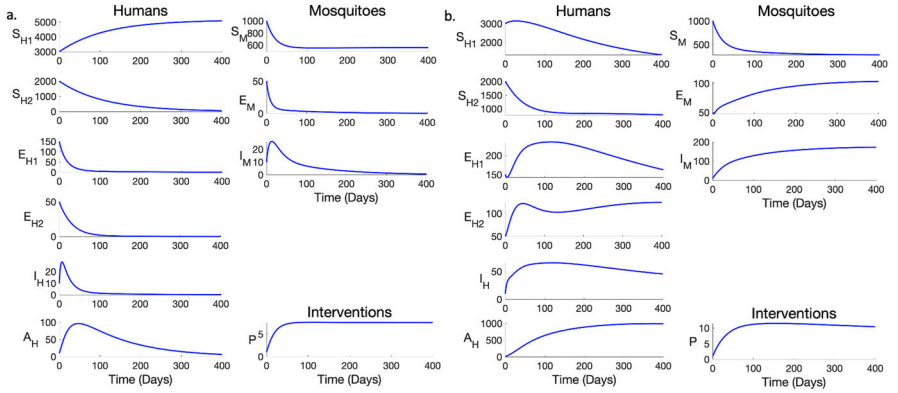


Fig. 6 Example model simulation results, showing human and mosquito population dynamics. a. Example simulation result of the model at $\mathcal{R}_c = 0.35$. b. Simulation result of the model at $\mathcal{R}_c = 2.26$. The baseline values given in Table 1 are employed as parameter values for the $\mathcal{R}_c < 1$ simulation result, while setting $\delta = 3$, $\psi_H = 0.5$ and $\psi_M = 0.5$ for the $\mathcal{R}_c > 1$ simulation. The initial conditions was set at $S_{H1}(0) = 3000$, $S_{H2}(0) = 2000$, $E_{H1}(0) = 150$, $E_{H2}(0) = 50$, $I_H(0) = 10$, $A_H(0) = 10$, $S_M(0) = 1000$, $E_M(0) = 50$, $I_M(0) = 10$, $P(0) = 1$

S_{H1} class that approaches the total human population size $\frac{\Lambda_H}{\mu_H}$. When one reconciles the behaviour with the description of the sub-classes, the disparity in the behaviours of the two susceptible sub-classes becomes clear; uninfected, non-immune humans make up the first susceptible class, whereas individuals in the second class are uninfected but partially immune, having acquired this immunity from a prior infection. Thus by inferring from the model diagram, Fig. 1, as I_H decreases towards the DFE, S_{H2} will decrease as well.

In Fig. 6b, where $\mathcal{R}_c > 1$, we observe a rise in the diseased classes of the model which shows that an increase in the number of infected mosquitoes has a corresponding effect on the number of infected humans and vice versa. In the susceptible curves however, there is sharp decline resulting from the dynamics in the infected compartment, and later an increase as individuals recover and as the model solution progresses towards equilibrium. The ripple effect of infection is supported here by the graphical results of the diseased and susceptible classes in Fig. 6b where an increase or decrease in the diseased classes of mosquitoes has a corresponding effect on the diseased classes of humans and vice versa.

A.3 Impact of Interventions During an Endemic Situation

We proceed to investigate the impact of the presence of interventions on an endemic situation. To do this, we run numerical simulations employing the baseline values given in Table 1 setting $\delta = 2$, $\psi_H = 0.5$ and $\psi_M = 0.5$. The endemic equilibrium was observed from time (years) 87 with approximately 272 infectious cases in the absence of interventions with $\mathcal{R}_0 = 9.05$, and 21 infectious cases in the presence of interventions with $\mathcal{R}_c = 2.08$ (Fig. 7a. and b.), and 0 cases in the presence of interventions with $\mathcal{R}_c = 0.74$ (Fig. 7c. and d.). Note that the dynamics in

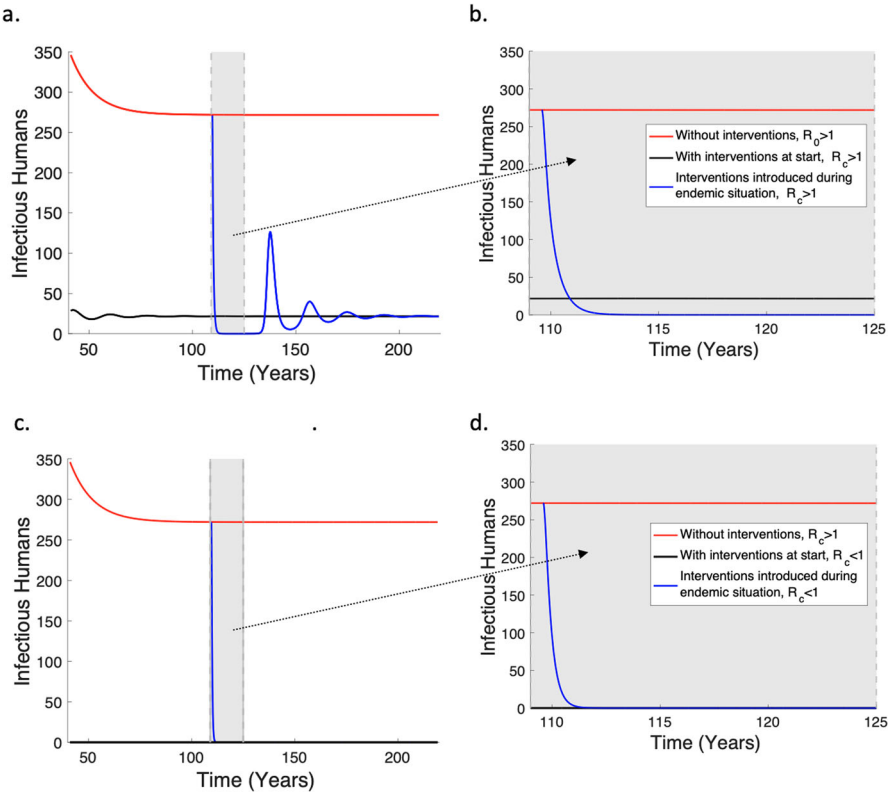


Fig. 7 Example simulation results exploring the impact of interventions on the human infectious population during an endemic situation. **a**. Simulation result of the infectious human population capturing the impact of the absence and presence of interventions from years 41 – 219 with $\mathcal{R}_0 = 9.05$ and $\mathcal{R}_c = 2.08$. **b.** A zoomed-in view of Fig. 7a. considering the dynamics in the infectious human population from time (years) 109 – 125 marked in the gray area and bounded by the gray dashed lines. **c**. A simulation result capturing the trajectory of the infectious human population during an endemic situation and demonstrating the impact of interventions in reducing the effective reproduction number ($\mathcal{R}_c$) below the threshold of 1, with $\mathcal{R}_0 = 9.05$ and $\mathcal{R}_c = 0.74$. **d.** A zoomed-in view of Fig. 7c. considering the dynamics in the infectious human population from time (years) 109 – 125 marked in the gray area and bounded by the gray dashed lines. The red solid line represents results in the infectious population in the absence of intervention and corresponds to $\mathcal{R}_0 = 9.05$, whereas the black solid line represents dynamics in the presence of interventions introduced at the start of the simulation at time 0 corresponding to $\mathcal{R}_c = 2.08$ in **a.** and **b.**, and $\mathcal{R}_c = 0.74$ in **c.** and **d.**. The blue solid line considers the dynamics after the introduction of interventions during an endemic situation with $\mathcal{R}_c = 2.08$ in **a.** and **b.**, and $\mathcal{R}_c = 0.74$ in **c.** and **d.**. These results were generated assuming initial conditions at $S_{H1}(0) = 3000$, $S_{H2}(0) = 2000$, $E_{H1}(0) = 150$, $E_{H2}(0) = 50$, $I_H(0) = 10$, $A_H(0) = 10$, $S_M(0) = 1000$, $E_M(0) = 50$, $I_M(0) = 10$, $P(0) = 0$ (Color figure online)

the absence of interventions were obtained by setting the intervention class to zero, as done in the baseline scenario of Sect. 4.3, see Table 3. At year 109, we introduced two classes of interventions to the endemic situation without interventions. The first class of interventions were assumed to reduce the number of cases during the endemic situation while still maintaining the effective reproduction number ($\mathcal{R}_c$) above the critical threshold of 1, (Fig. 7a.and b.). These interventions were introduced

in the model by setting the intervention-related parameters to the baseline values provided in Table 1,($\eta = 0.3, \kappa = 0.04, \xi = 0.0025, b = 0.5, c = 0.4$). The second class of interventions were aimed to bring the $\mathcal{R}_c$ threshold below 1 by setting $\eta = 0.5, \kappa = 0.02, \xi = 0.0025, b = 0.5$ and $c = 0.4$ (see Fig. 7c. and d.). In Fig. 7 we present a summary of our results from this study.

From Fig. 7a. and b., it is evident that the implementation of interventions during a period of heightened disease (endemic) prevalence led to a decrease in the number of infectious human cases, from approximately 272 cases to 21 cases at equilibrium. In Fig. 7 b. we provide a focused view of the dynamics of the infectious human class during years 109 – 125 and observe a decline in infectious cases in the first 6 years after the introduction of interventions. Infectious cases reduce from about 272 in year 109 to $I < \epsilon = 0.3$ in year 113. This reduced transmission is sustained for about 16 years, that is until year 129. Following year 129, there is a resurgence in infectious cases, accompanied by fluctuations, as the dynamics (depicted by the blue solid line, Fig. 7a. and b.) converge towards the endemic situation (depicted by the black solid line, Fig. 7a. and b.) with interventions implemented from the outset.

In Fig. 7 c. and d., we explore the potential of interventions in lowering the $\mathcal{R}_c$ threshold below 1. Our analysis reveals that the introduction of these interventions leads to a more rapid decline in the number of infectious cases, reaching $I < \epsilon = 0.3$ by year 111. This level of infectious cases is maintained as the system reaches equilibrium, with $\mathcal{R}_c = 0.74$. The potential for malaria elimination during the period where $I < \epsilon$ could have been explored and predicted using a stochastic model. However, due to the limitation of employing a continuous model, we are unable to predict malaria elimination accurately during this period.

Acknowledgements We gratefully acknowledge the support of the Melbourne Research Scholarship, the National Institute of Allergy and Infectious Diseases and the National Institutes of Health for their financial assistance, enabling the completion of this research.

Author Contributions MAK, STJ, JAF and CRW conceived the study. MAK conducted the simulations and drafted the manuscript. KET and KPD provided feedback on the modelling of the asymptomatic class and the malaria control interventions considered in the study. STJ, KET and KPD critically reviewed and revised the manuscript for intellectual content. JAF, and CRW oversaw project coordination and contributed to the manuscript revisions. All authors read and approved the final manuscript.

Funding Open Access funding enabled and organized by CAUL and its Member Institutions This research was supported by a Melbourne Research Scholarship awarded to M. A. Korsah, and the National Institute of Allergy and Infectious Diseases, National Institutes of Health through the joint NIH-NSF-NIFA Ecology and Evolution of Infectious Disease award R01-AI149779 to K. P. Day. J. A. Flegg's research is supported by the ARC (DP200100747, FT210100034) and the National Health and Medical Research Council (APP2019093).

Data Availibility Data sharing does not apply to this paper, as there were no generated or analyzed data sets during the study.

Open Access This article is licensed under a Creative Commons Attribution 4.0 International License, which permits use, sharing, adaptation, distribution and reproduction in any medium or format, as long as you give appropriate credit to the original author(s) and the source, provide a link to the Creative Commons licence, and indicate if changes were made. The images or other third party material in this article are included in the article's Creative Commons licence, unless indicated otherwise in a credit line to the material. If material is not included in the article's Creative Commons licence and your intended use is not permitted

by statutory regulation or exceeds the permitted use, you will need to obtain permission directly from the copyright holder. To view a copy of this licence, visit http://creativecommons.org/licenses/by/4.0/.

References

Accrombessi M, Cook J, Dangbenon E, Sovi A, Yovogan B, Assongba L, Adoha CJ, Akinro B, Affoukou C, Padonou GG, et al (2024) Effectiveness of pyriproxyfen-pyrethroid and chlorfenapyr-pyrethroid long-lasting insecticidal nets (LLINs) compared with pyrethroid-only LLINs for malaria control in the third year post-distribution: a secondary analysis of a cluster-randomised controlled trial in Benin. Lancet Infect Dis

Agyemang-Badu SY, Awuah E, Oduro-Kwarteng S, Dzamesi JYW, Dom NC, Kanno GG (2023) Environmental Management and sanitation as a malaria vector control strategy: a qualitative cross-sectional study among stakeholders, Sunyani Municipality, Ghana. Environ Health Insights 17:11786302221146890

Ahmad A, Mohammed NI, Joof F, Affara M, Jawara M, Abubakar I, Okebe J, Ceesay S, Hamid-Adiamoh M, Bradley J et al (2023) Asymptomatic Plasmodium falciparum carriage and clinical disease: a 5-year community-based longitudinal study in The Gambia. Malaria J 22(1):82

Alves FP, Gil LHS, Marrelli MT, Ribolla PE, Camargo EP, Da Silva LHP (2005) Asymptomatic carriers of Plasmodium spp. as infection source for malaria vector mosquitoes in the Brazilian Amazon. J Med Entomol 42(5):777–779

Baihaqi MA, Adi-Kusumo F (2020) Modelling malaria transmission in a population with SEIRS p method. In: AIP conference proceedings, vol 2264, p 020002, AIP Publishing LLC

Casares S, Brumeanu T-D, Richie TL (2010) The RTS, S malaria vaccine. Vaccine 28(31):4880–4894

Castro MC, Tsuruta A, Kanamori S, Kannady K, Mkude S (2009) Community-based environmental management for malaria control: evidence from a small-scale intervention in Dar es Salaam, Tanzania. Malaria J 8:1–11

Center for Disease Control and Prevention. About Malaria. July 2020. Accessed: 15-02-2022

Chitnis N (2005) Using mathematical models in controlling the spread of malaria [Ph. D. thesis]. Tucson: Program in Applied Mathematics,, University of Arizona

Chitnis N, Cushing JM, Hyman J (2006) Bifurcation analysis of a mathematical model for malaria transmission. SIAM J Appl Math 67(1):24–45

Chitnis N, Hyman JM, Cushing JM (2008) Determining important parameters in the spread of malaria through the sensitivity analysis of a mathematical model. Bull Math Biol 70(5):1272–1296

Chitnis N, Schapira A, Smith T, Steketee R (2010) Comparing the effectiveness of malaria vector-control interventions through a mathematical model. Am J Trop Med Hygiene 83(2):230

Dengela D, Seyoum A, Lucas B, Johns B, George K, Belemvire A, Caranci A, Norris LC, Fornadel CM (2018) Multi-country assessment of residual bio-efficacy of insecticides used for indoor residual spraying in malaria control on different surface types: results from program monitoring in 17 PMI/USAID-supported IRS countries. Parasites Vectors 11(1):1–14

Diekmann O, Heesterbeek JAP, Metz JA (1990) On the definition and the computation of the basic reproduction ratio R 0 in models for infectious diseases in heterogeneous populations. J Math Biol 28(4):365–382

Diptyanusa A, Zablon KN (2020) Addressing budget reduction and reallocation on health-related resources during COVID-19 pandemic in malaria-endemic countries. Malaria J 19(1):1–4

Enahoro I, Eikenberry S, Gumel AB, Huijben S, Paaijmans K (2020) Long-lasting insecticidal nets and the quest for malaria eradication: a mathematical modeling approach. J Math Biol 81(1):113–158

Fongnikin A, Houeto N, Agbevo A, Odjo A, Syme T, N'Guessan R, Ngufor C (2020) Efficacy of Fludora® Fusion (a mixture of deltamethrin and clothianidin) for indoor residual spraying against pyrethroid-resistant malaria vectors: laboratory and experimental hut evaluation. Parasites Vectors 13:1–11

Gari T, Lindtjørn B (2018) Reshaping the vector control strategy for malaria elimination in Ethiopia in the context of current evidence and new tools: opportunities and challenges. Malaria J 17(1):1–8

Gogue C, Wagman J, Tynuv K, Saibu A, Yihdego Y, Malm K, Mohamed W, Akplu W, Tagoe T, Ofosu A et al (2020) An observational analysis of the impact of indoor residual spraying in Northern, Upper East,, and Upper West regions of Ghana: 2014 through 2017. Malaria J 19:1–13

Grassly NC, Fraser C (2008) Mathematical models of infectious disease transmission. Nat Rev Microbiol 6(6):477–487

Griffin JT, Hollingsworth TD, Okell LC, Churcher TS, White M, Hinsley W, Bousema T, Drakeley CJ, Ferguson NM, Basáñez M-G et al (2010) Reducing *plasmodium* falciparum malaria transmission in Africa: a model-based evaluation of intervention strategies. PLOS Med 7(8):e1000324

Hakizimana D, Ntizimira C, Mbituyumuremyi A, Hakizimana E, Mahmoud H, Birindabagabo P, Musanabaganwa C, Gashumba D (2022) The impact of Covid-19 on malaria services in three high-endemic districts in Rwanda: a mixed-method study. Malaria J 21(1):48

Haldar K, Bhattacharjee S, Safeukui I (2018) Drug resistance in Plasmodium. Nat Rev Microbiol 16(3):156–170

Hogan AB, Jewell BL, Sherrard-Smith E, Vesga JF, Watson OJ, Whittaker C, Hamlet A, Smith JA, Winskill P, Verity R et al (2020) Potential impact of the COVID-19 pandemic on HIV, tuberculosis, and malaria in low-income and middle-income countries: a modelling study. Lancet Global Health 8(9):e1132–e1141

Jiram AI, Ooi CH, Rubio JM, Hisam S, Karnan G, Sukor NM, Artic MM, Ismail NP, Alias NW (2019) Evidence of asymptomatic submicroscopic malaria in low transmission areas in Belaga district, Kapit division, Sarawak, Malaysia. Malaria J 18(1):1–12

Jun F, Li Z, Hong T, Shui-sen Z, Zhi-gui X (2021) From elimination to post-elimination: characteristics, challenges and re-transmission preventing strategy of imported malaria in China. China Trop Med 21(1):2021

Kateera F, Ingabire CM, Hakizimana E, Rulisa A, Karinda P, Grobusch MP, Mutesa L, van Vugt M, Mens PF (2015) Long-lasting insecticidal net source, ownership and use in the context of universal coverage: a household survey in eastern Rwanda. Malaria J 14:1–10

Kilian A, Obi E, Mansiangi P, Abílio AP, Haji KA, Blaufuss S, Olapeju B, Babalola S, Koenker H (2021) Variation of physical durability between LLIN products and net use environments: summary of findings from four African countries. Malaria J 20(1):1–11

Kim S, Luande VN, Rocklöv J, Carlton JM, Tozan Y (2021) A systematic review of the evidence on the effectiveness and cost-effectiveness of mass screen-and-treat interventions for malaria control. Am J Trop Med Hygiene 105(6):1722

Korsah M (2021) Assessment of the impact of awareness programs on the transmission dynamics of COVID-19. May 2021. Available at https://scholar.utc.edu

Li MY (2018) An introduction to mathematical modeling of infectious diseases, vol 2. Springer

Lin JT, Saunders DL, Meshnick SR (2014) The role of submicroscopic parasitemia in malaria transmission: What is the evidence? Trends Parasitol 30(4):183–190

Mojeeb A, Adu IK, Yang C (2017) A simple seir mathematical model of malaria transmission. Asia Res J Math, pp 1–27

Musa JJ, Moore SJ, Moore J, Mbuba E, Mbeyela E, Kobe D, Swai JK, Odufuwa OG (2020) Long-lasting insecticidal nets retain bio-efficacy after 5 years of storage: implications for malaria control programmes. Malaria J 19:1–12

Nguyen TD (2016) The effects of different deployment strategies of artemisinin combination therapies on slowing down the spread of antimalarial drug resistence: investigation with individual-based simulations. Open University (United Kingdom)

Ngwa GA, Shu WS (2000) A mathematical model for endemic malaria with variable human and mosquito populations. Math Comput Modell 32(7–8):747–763

Obabiyi O, Olaniyi S (2019) Global stability analysis of malaria transmission dynamics with vigilant compartment. Electronic J Differ Equ, pp 1–10

Obembe A, Anyaele OO, Oduola AO (2014) Lessons from the implementation of LLIN distribution campaign in Ilorin Kwara State, Nigeria. BMC Public Health 14:1–8

Ojuka P, Boum Y, Denoeud-Ndam L, Nabasumba C, Muller Y, Okia M, Mwanga-Amumpaire J, De Beaudrap P, Protopopoff N, Etard J-F (2015) Early biting and insecticide resistance in the malaria vector Anopheles might compromise the effectiveness of vector control intervention in Southwestern Uganda. Malaria J 14:1–8

Okiring J, Gonahasa S, Nassali M, Namuganga JF, Bagala I, Maiteki-Sebuguzi C, Opigo J, Nabende I, Nangendo J, Kabami J et al (2022) LLIN Evaluation in Uganda Project (LLINEUP2)-factors associated with coverage and use of long-lasting insecticidal nets following the 2020–21 national mass distribution campaign: a cross-sectional survey of 12 districts. Malaria J 21(1):293

Olaniyi S, Okosun K, Adesanya S, Lebelo R (2020) Modelling malaria dynamics with partial immunity and protected travellers: optimal control and cost-effectiveness analysis. J Biol Dyn 14(1):90–115
Perkins DJ, Were T, Davenport GC, Kempaiah P, Hittner JB, Ong'echa JM (2011) Severe malarial anemia: innate immunity and pathogenesis. Int J Biol Sci 7(9):1427
Plowe CV (2022) Malaria chemoprevention and drug resistance: a review of the literature and policy implications. Malaria J 21(1):104
Pryce RMJ, Lengeler C (2018) Insecticide-treated nets for preventing malaria. Cochrane Database Systemat Rev, 11
Pryce J, Medley N, Choi L (2022) Indoor residual spraying for preventing malaria in communities using insecticide-treated nets. Cochrane Database Systemat Rev, 1
Raghavendra K, Chourasia MK, Swain DK, Bhatt RM, Uragayala S, Dutta G, Kleinschmidt I (2017) Monitoring of long-lasting insecticidal nets (LLINs) coverage versus utilization: a community-based survey in malaria endemic villages of Central India. Malaria J 16:1–8
Rehman AM, Coleman M, Schwabe C, Baltazar G, Matias A, Roncon Gomes I, Yellott L, Aragon C, Nseng Nchama G, Mzilahowa T et al (2011) How much does malaria vector control quality matter: the epidemiological impact of holed nets and inadequate indoor residual spraying. PLOS One 6(4):e19205
Roberts L et al (2021) How COVID is derailing the fight against HIV, TB and malaria. Nature 597(7876):314
Rodrigues HS, Monteiro MTT, Torres DF (2013) Sensitivity analysis in a dengue epidemiological model. In: Conference papers in science, vol 2013, Hindawi
Rogerson SJ, Beeson JG, Laman M, Poespoprodjo JR, William T, Simpson JA, Price RN (2020) Identifying and combating the impacts of COVID-19 on malaria. BMC Med 18(1):1–7
Rono MK, Nyonda MA, Simam JJ, Ngoi JM, Mok S, Kortok MM, Abdullah AS, Elfaki MM, Waitumbi JN, El-Hassan IM et al (2018) Adaptation of Plasmodium falciparum to its transmission environment. Nat Ecol Evol 2(2):377–387
Shah NH, Gupta J (2013) SEIR model and simulation for vector borne diseases. Appl Math
Sherrard-Smith E, Griffin JT, Winskill P, Corbel V, Pennetier C, Djénontin A, Moore S, Richardson JH, Müller P, Edi C et al (2018) Systematic review of indoor residual spray efficacy and effectiveness against Plasmodium falciparum in Africa. Nat Commun 9(1):4982
Shretta R, Avanceña AL, Hatefi A (2016) The economics of malaria control and elimination: a systematic review. Malaria J 15(1):1–14
Shretta R, Silal SP, Malm K, Mohammed W, Narh J, Piccinini D, Bertram K, Rockwood J, Lynch M (2020) Estimating the risk of declining funding for malaria in Ghana: the case for continued investment in the malaria response. Malaria J 19(1):1–15
Stopard IJ, Churcher TS, Lambert B (2021) Estimating the extrinsic incubation period of malaria using a mechanistic model of sporogony. PLOS Comput Biol 17(2):e1008658
Tan KR, Coleman J, Smith B, Hamainza B, Katebe-Sakala C, Kean C, Kowal A, Vanden Eng J, Parris TK, Mapp CT et al (2016) A longitudinal study of the durability of long-lasting insecticidal nets in Zambia. Malaria J 15:1–12
Tapera O (2019) Determinants of long-lasting insecticidal net ownership and utilization in malaria transmission regions: evidence from Zimbabwe demographic and health surveys. Malaria J 18:1–7
Tiedje KE, Oduro AR, Agongo G, Anyorigiya T, Azongo D, Awine T, Ghansah A, Pascual M, Koram KA, Day KP (2017) Seasonal variation in the epidemiology of asymptomatic Plasmodium falciparum infections across two catchment areas in Bongo District, Ghana. Am J Trop Med Hygiene 97(1):199
Trampuz A, Jereb M, Muzlovic I, Prabhu RM (2003) Clinical review: Severe malaria. Critical Care 7(4):1–9
Tumwiine J, Mugisha JY, Luboobi LS (2008) Threshold and stability results for a malaria model in a population with protective intervention among high-risk groups. Math Modell Anal 13(3):443–460
Turner , Jung C, Tan P, Gotika S, Mago V (2015) A comprehensive model of spread of malaria in humans and mosquitos. In: SoutheastCon, pp 1–6, IEEE, 2015
ul Rehman A, Singh R, Singh J (2022) Mathematical analysis of multi-compartmental malaria transmission model with reinfection. Chaos Solitons Fractals, vol 163, p 112527
Van den Driessche P, Watmough J (2002) Reproduction numbers and sub-threshold endemic equilibria for compartmental models of disease transmission. Math Biosci 180(1–2):29–48
Waltmann A, Darcy AW, Harris I, Koepfli C, Lodo J, Vahi V, Piziki D, Shanks GD, Barry AE, Whittaker M et al (2015) High rates of asymptomatic, sub-microscopic Plasmodium vivax infection and disappearing Plasmodium falciparum malaria in an area of low transmission in Solomon Islands. PLOS Neglected Tropical Diseases 9(5):e0003758

Weiss DJ, Bertozzi-Villa A, Rumisha SF, Amratia P, Arambepola R, Battle KE, Cameron E, Chestnutt E, Gibson HS, Harris J et al (2021) Indirect effects of the COVID-19 pandemic on malaria intervention coverage, morbidity, and mortality in Africa: a geospatial modelling analysis. Lancet Infect Dis 21(1):59–69

Woldegerima WA, Ouifki R, Banasiak J (2021) Mathematical analysis of the impact of transmission-blocking drugs on the population dynamics of malaria. Appl Math Comput 400:126005

World Health Organization et al (2021) WHO guidelines for malaria, 13 July 2021. tech. rep., World Health Organization

World Health Organization (2018) Global report on insecticide resistance in malaria vectors: 2010–2016

World Health Organization (2019) "World Malaria Report 2019" at a glance. December 2019. Accessed: 10-03-2022

World Health Organization (2021) Global Malaria Programme, June 2021. Accessed: 14-02-2022

World Health Organization (2021) WHO Malaria Terminology, 2021 update. Accessed: 14-02-2022

World Health Organization and others (2022) World Malaria Report 2022. World Health Organization

Worrall E, Connor S, Thomson M (2007) A model to simulate the impact of timing, coverage and transmission intensity on the effectiveness of indoor residual spraying (IRS) for malaria control. Trop Med Int Health 12(1):75–88

Wubishet MK, Berhe G, Adissu A, Tafa MS (2021) Effectiveness of long-lasting insecticidal nets in prevention of malaria among individuals visiting health centres in Ziway-Dugda District, Ethiopia: matched case-control study. Malaria J 20(1):1–15

Wu H, Hu Z (2021) Malaria transmission model with transmission-blocking drugs and a time delay. Math Prob Eng, vol 2021

Yang HM, Ferreira MU (2000) Assessing the effects of global warming and local social and economic conditions on the malaria transmission. Revista de Saude Publica 34(3):214–222

Yang C, Wang X, Gao D, Wang J (2017) Impact of awareness programs on cholera dynamics: two modeling approaches. Bull Math Biol 79(9):2109–2131

Publisher's Note Springer Nature remains neutral with regard to jurisdictional claims in published maps and institutional affiliations.